

GCr15 Bearing Steel Metallographic Image Fine Segmentation Model Based on Transformer Unet Network and CV model

Hanyu Zhang^{1,2}, Lixin Tang¹ and Yong Shuai³

¹ National Frontiers Science Center for Industrial Intelligence and Systems Optimization, Northeastern University, Shenyang, 110819, China

² Key Laboratory of Data Analytics and Optimization for Smart Industry (Northeastern University), Ministry of Education, Shenyang, 110819, China.

³ Jiangxi Xinyu Iron and Steel Group Co., Ltd, Xinyu, 338000, China.

Abstract. GCr15 bearing steel metallographic image of the proportion of insoluble carbides, the size and distribution of uniformity is an important indicator to evaluate the quality of bearing steel. **Insufficient edge definition of insoluble carbide particles, complex interlacing of lamellar and spherical carbide imaging edge**, and difficulty in accurate segmentation of carbides with small size lead to the challenging problem of automatically extracting insoluble carbides from low-quality metallurgical images. In this paper, we propose a novel two-stage model combining Transformer Unet (TUnet) and Chan-Vase (CV), TUnet-CV, for metallographic image fine segmentation. In the coarse segmentation stage, TUnet model is used to obtain the complex topology of the lamellar carbides. The coarse segmentation probability map obtained by the neural network is as a priori information to the fine segmentation stage. In the fine segmentation stage, the carbides with smaller particle size are finely segmented by an improved CV model. The proposed model reaches Dice coefficient of 0.9238 on the GCr15 bearing steel metallographic dataset. The experimental results demonstrate the effectiveness of each component in the proposed model.

Keywords: GCr15 bearing steel, Metallographic image segmentation, insoluble carbides, Transformer Unet, CV model.

1 Introduction

GCr15 is a high-carbon chromium bearing steel commonly used in industry. The insoluble carbide content of GCr15 bearing steel should be kept within a specific range. The content is too high will reduce the fatigue life of bearing steel, and too low will decrease the surface wear resistance of bearing steel. In order to maintain a uniform organization of bearing steel. The content of banded carbide and reticulated carbide phases in the organization should be minimized, they seriously affect the performance and life of bearing steel. The particles of insoluble carbide in bearing steel require high roundness, small and regular shape. When there are irregular particles, the heat

treatment effect, fatigue life and service life of bearing steel will be affected. Therefore, the segmentation of metallographic images of insoluble carbides and their quantitative analysis are of great importance to measure the performance of GCr15 bearing steel.

Metallographic analysis is an important technical tool for understanding the intrinsic structure of materials. Typically, metallographic images are identified, measured and analyzed by human experts, including grain size, area ratio, percentage and homogeneity of each constituent phase in a multiphase alloy. Relationships between organization, properties and composition are then established. This is a subjective, labor-intensive process with poor repeatability. Therefore, the study of computer-aided metallographic analysis has become the focus of many researchers. Digital image processing techniques are used to extract features, identify, segment and quantify microstructural features.

Metallographic segmentation methods can be classified into two groups: unsupervised methods and supervised methods. Unsupervised methods use the intrinsic association between image features to identify target and segment images without training on manually labeled datasets. Dominguez-Rodriguez et al. [1] used the Sobel operator to identify the edge and the threshold method to discretize the edge. The phase is selected by averaging the color of each segmented particle. Cipolloni et al. [2] used image analysis method to systematically describe the sintered body and surface porosity of chrome-molybdenum low-alloy steel. Prediction of tensile force based on image feature data. Martyushev [3] developed a micro-structure image processing software for quantitative metallographic analysis of digital images of material microstructure. The software can calculate the volume fraction and average particle size of the structure in a field of view by secant theorem. Dutta [4] used Otsu threshold algorithm to segment microscopic images of biphasic steel generated by ferrite and martensite two-phase optical microscopy. Hecht et al. [5] used ImageJ software to divide carbide network, and this method requires a good grasp of the relevant application of its software. Although these methods have shown promising results, they encounter problems such as noise sensitivity, unpredictable thresholds, and difficulty in considering geometric information in segmentation. Chan et al. [6] proposed the Chan-Vese (CV) model based on the level set method, which showed better results in the metallographic segmentation task. At present, many researchers carry out research based on this model. However, the model is sensitive to the initial contour and noise, and the selection of the initial contour directly affects the final segmentation result.

Supervised methods require training the classifier using manually labeled real data for the classification task. In the past few years, the methods based on deep learning have been rapidly developed [14]-[19]. Naik [7] proposed a supervised machine learning approach to identify phases (ferrite, pearlite, and martensite) in metallurgical ASTM A36 heat-treated steel. Kusche et al. [8] researched the damage mechanism of biphasic steel and used convolutional neural network to classify the damage mechanism with high resolution. DeCost [9] combined the supervised and the unsupervised methods to classify a subset of high carbon steel microstructure using convolutional neural networks. Ronneberger O et al. [10] proposed the U-net depth segmentation network, which has been widely used in the field of segmentation. It innovatively

proposed a U shaped network structure combining coding and decoding to integrate multi-level semantic information of images. Sha et al. [11] proposed an improved Unet model, TUnet, which introduced the multi-head attention mechanism in the encoder to capture global information of the image. Although the model based on deep learning performs well in the field of metallographic segmentation, the limited number of metallographic images and the complex topology structure leading to poor segmentation accuracy at local complex target boundaries and segmentation of small targets.

The following difficulties exist in segmenting the insoluble carbides in the metallographic images of GCr15 bearing steel. **Firstly, the contained insoluble austenite, martensite, and insoluble carbide particles are similar in color when imaged by the microscope, so they have very similar grayscale values during image processing.** Secondly, the edges of insoluble carbide particles are not clear enough, and the lamellar carbides are intermingled with the spherical carbides. Thirdly, the carbides with small particle size are difficult to be divided accurately. Considering the above problems, a two-stage bearing steel fine segmentation model TUnet-CV is proposed in this paper. In the coarse segmentation stage, we select the TUnet network to segment the larger lamellar carbons and capture their complex topology by convolutional operations with a multi-headed attention mechanism. The coarse segmentation probability map obtained by the neural network is fed as a priori information to the fine segmentation stage. In the fine segmentation stage, the carbides with smaller particle size are finely segmented by a CV model with the probability map introduced as the initial contour. The proposed model is tested on the GCr15 bearing steel metallographic dataset. The experimental results demonstrate the validity of each component of the proposed model.

Our main contributions can be summarized as follows:

- 1) We propose a novel two-stage model TUnet-CV for bearing steel metallographic image segmentation including coarse segmentation and fine segmentation.
- 2) We propose a Transformer Unet neural network to segment the lamellar carbons in the coarse segmentation stage, and the probability map obtained through the network is passed to the fine segmentation stage as a priori information.
- 3) We propose an improved CV model that introduces probability maps as the initial contour for the segmentation of the carbides with smaller particle size in the fine stage.
- 4) We demonstrate experiment results on the GCr15 bearing steel metallographic dataset, experimental results show the effectiveness of the proposed method.

The remainder of the paper is structured as follows: Section 2 introduces the U-net model architecture and the CV model. Our proposed model is described in Section 3. Section 4 describes the experimental setup and results. Section 5 is a summary of the entire work.

2 Related Work

2.1 U-net

U-net is a popular network in the field of semantic segmentation and is suitable for small sample datasets. The U-net network diagram is presented in Figure 1.

The U-net network is a symmetric U-shaped structure containing two parts: encoding and decoding. The left part is the encoder part, which consists of convolution operations and downsampling operations. A total of five times of the above operations are performed, and the obtained feature maps are fed to the decoder part in the right part. The decoder part consists of the convolution operation and the upsampling operation. In the upsampling operation, a bilinear interpolation method is chosen. In the last layer of the decoder, the probability map of the image prediction is obtained, where 0.5 to 1 represents the foreground region and 0 to 0.5 represents the background region.

The U-net network connects the feature map of the encoder part with the feature map of the decoder part by a join operation, which enables the fusion of the underlying location information with the semantic information of the deeper features. The structure is simple and stable, which is well suited for small sample datasets. Because of the small amount of metallographic image sample data, the interlacing of multiple organizations leading to blurred boundaries, and the lack of semantic information due to fixed organizational structure, both high-level semantic information and low-level features are important. The connection operation and U-shaped structure of the U-net network are exactly suitable for solving the above problems, so the U-net neural network is chosen as the basic structure for metallographic image segmentation of bearing steel in this paper.

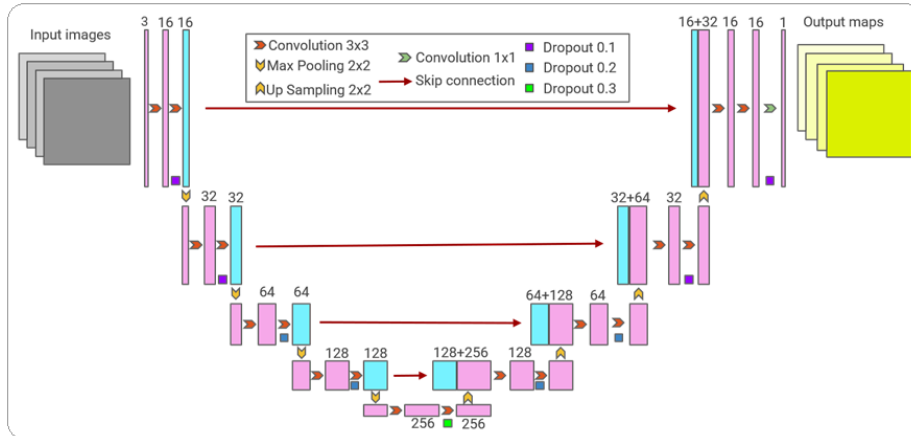


Fig. 1. U-net network structure.

2.2 CV model

D. Mumford and J. Shah first proposed a classical active contour model based on region segmentation (MS model) [12], which can accomplish image segmentation while also accomplishing image region smoothing operations, and the model is easy to compute numerically. However, the model still has certain problems that can make the segmentation less effective, such as the excessive running time required, the excessive dependence on the length parameter and the fact that since the energy function is nonconvex, it is more difficult to obtain global-based minima, and local-based minima are usually obtained.

To improve the problems of the MS model, Chan and Vese simplified their energy function and proposed the CV model with an energy functional defined as:

$$\begin{aligned}
 E^{CV}(C, c_1, c_2) = & \lambda_1 \iint_{inside(C)} |u_0(x, y) - c_1|^2 dx dy \\
 & + \lambda_2 \iint_{outside(C)} |u_0(x, y) - c_2|^2 dx dy \\
 & + \mu \cdot Length(C) + \nu \cdot Area(inside(C))
 \end{aligned} \tag{1}$$

where $inside(C)$ and $outside(C)$ represent the inner and outer regions of the image curve, respectively. c_1 and c_2 represent the grayscale values of the two image regions. $Length(C)$ is the arc length of the boundary curve, and $Area(inside(c))$ is the area of the inner region of the curve. $\lambda_1, \lambda_2, \mu, \nu$ are positive parameters. The evolutionary contour C is denoted by the zero level set of the level set function:

$$\begin{cases}
 C = \{(x, y) \in \Omega : \phi(x, y) = 0\} \\
 inside(C) = \{(x, y) \in \Omega : \phi(x, y) > 0\} \\
 outside(C) = \{(x, y) \in \Omega : \phi(x, y) < 0\}
 \end{cases} \tag{2}$$

The CV model also introduces a regularized Heaviside function $H(u)$ and Dirac function $\delta(u)$:

$$\nabla H(u) = \delta(u) \nabla u, \quad \delta(u) = \frac{dH(u)}{du} \tag{3}$$

Transforming each term in the energy functional (1) into a new energy function:

$$\begin{aligned}
 E^{CV}(c_1, c_2, \phi) = & \lambda_1 \int_{\Omega} |u_0(x, y) - c_1|^2 H(\phi(x, y)) dx dy \\
 & + \lambda_2 \int_{\Omega} |u_0(x, y) - c_2|^2 (1 - H(\phi(x, y))) dx dy \\
 & + \mu \int_{\Omega} \delta(\phi(x, y)) |\nabla \phi(x, y)| dx dy + \nu \int_{\Omega} H(\phi(x, y)) dx dy
 \end{aligned} \tag{4}$$

c_1 and c_2 can be computed for a constant level set function ϕ :

$$\begin{cases} c_1(\phi) = \frac{\int_{\Omega} u_0(x, y)H(\phi(x, y))dxdy}{\int_{\Omega} H(\phi(x, y))dxdy} \\ c_2(\phi) = \frac{\int_{\Omega} u_0(x, y)(1-H(\phi(x, y)))dxdy}{\int_{\Omega} (1-H(\phi(x, y)))dxdy} \end{cases} \quad (5)$$

Keep c_1 and c_2 constant so that the energy function E^{CV} is minimized by the gradient descent flow method:

$$\frac{\partial \varphi}{\partial t} = \delta_{\varepsilon}(\varphi) \left[\mu \operatorname{div} \left(\frac{\nabla \varphi}{|\nabla \varphi|} \right) - \nu - \lambda_1 (u_0 - c_1)^2 + \lambda_2 (u_0 - c_2)^2 \right] \quad (6)$$

3 Methodology

The framework of the proposed TUnet-CV model is depicted in Figure 2. The proposed model consists of two stages, coarse segmentation and fine segmentation. First, in the coarse segmentation stage, a TUnet neural network is used to extract the complex topology of the lamellar carbide image. A probability map of the coarse segmentation results is obtained by this network. Next, the probability map is introduced into the CV model as an initial contour to segment the smaller size carbides in the fine segmentation stage.

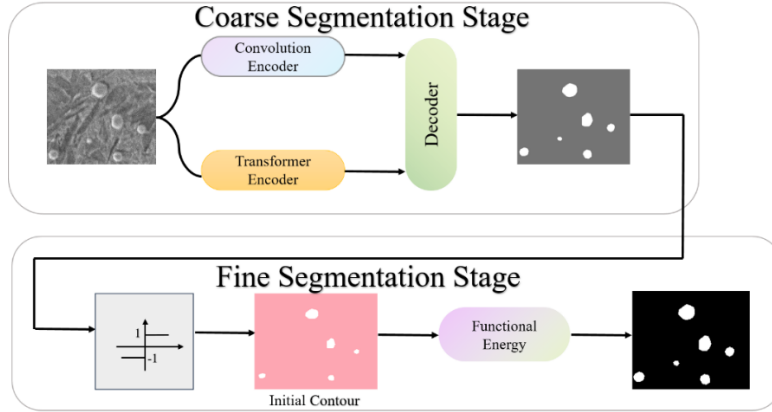


Fig. 2. The TUnet-CV model overall structure.

3.1 Coarse Segmentation Stage

In this section, the TUnet neural network applied in this paper is shown in Figure 3. The network is based on the structure of the U-net network with the transformer

module embedded in the encoding part. The coarse segmentation results as well as the predicted probability maps are obtained through the network.

The transformer module introduced in this paper refers to the Transformer block inserted in the original image. In Figure 3, the input to the transformer module needs to be sequential data. Therefore, the original retinal images need to be sprawled into arrays. Characteristic maps output by the Transformer Encoder section have feature maps with different receptive domains. Then, they are reshaped to be matched with the size of the U-net Encoder feature map and are passed directly to the decoder. Finally, they are attached to the decoder feature map to ensure that the decoder input contains multi-level metallic image information, which is more conducive to the network prediction.

In the metallographic images of bearing steel, the insoluble carbides are similar to the insoluble austenite and martensite structures and the lamellar carbides are intermingled with the spherical carbides, so the complex topology of the lamellar carbides can be effectively obtained by the convolution operation with the multi-head attention mechanism in the transformer module. However, due to the small amount of data and complex structure of bearing steel metallographic images, the carbides with small size are not easily perceived by the network, resulting in the poor segmentation of the neural network at the smaller carbides. To obtain the segmentation results of fine insoluble carbides, the probability map is obtained as the initial contour through the final softmax layer of the network. The initial contour is embedded as a priori information in the CV model of the fine stage segmentation phase.

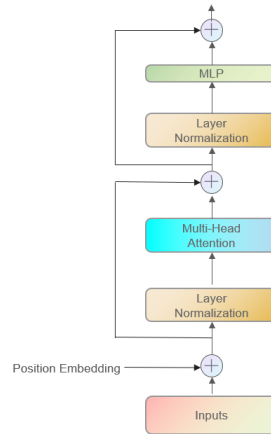


Fig. 3. Transformer module.

3.2 Fine Segmentation Stage

In this section, an improved CV model with probability map as the initial contour is proposed for the fine segmentation of bearing steel metallographic images. The CV model is a level set model based on energy fitting, in which the initial contour is em-

bedded as a priori information can effectively solve its sensitivity to the initial contour, and the iteration speed is better improved.

Assume that the bearing steel metallographic image is represented as μ . ϕ_{ini} represents the initial contour of the level set. The proposed modified CV model functional formula is shown as (7):

$$\begin{cases} E(\phi, P) = E_{\text{data}} + \nu \int |\nabla H_\varepsilon(\zeta(x))| dx + \mu P(\zeta) \\ \phi(0, x, y) = \phi_{\text{ini}}(x, y) \end{cases} \quad (7)$$

where E_{data} is the data term and the formula is shown as (8):

$$\begin{aligned} E_{\text{data}}(\phi, c_1, c_2) = & \lambda_1 \int_{\Omega} |u_0(x, y) - c_1|^2 H(\phi(x, y)) dx dy \\ & + \lambda_2 \int_{\Omega} |u_0(x, y) - c_2|^2 (1 - H(\phi(x, y))) dx dy \end{aligned} \quad (8)$$

According to the E-L equation, the partial differential equation as shown in Equation (6) can be obtained. The above partial differential equation is solved by the finite difference method with the iterative formula:

$$\phi^t = \phi^{t-1} + \Delta t \frac{\partial \phi^{t-1}}{\partial t} \quad (9)$$

The CV model is sensitive to the initial contours, and usually different segmentation results are produced due to the difference in the initial contours. In this paper, the bearing steel metallographic probability map is finally obtained in the coarse segmentation stage. This probability map is used as the initial contour of the CV model in the fine segmentation stage. Since this map already has the coarse segmentation results, it is used as a powerful priori information to guide the contraction and expansion of the CV model during the segmentation process, directly guiding the contour iterations toward energy minimization. As a result, the efficiency of the CV model is greatly improved. In the experimental section, the number of iterations of the CV model with the introduction of a priori information will be compared with the normal CV model.

4 Experiments and Analysis

4.1 Implementation details

In this section, this paper takes GCr15 tapered roller bearings after quenching and heat treatment as the experimental research object [13]. Ma et al. [20] calculated the iron-carbon phase diagram of GCr15 bearing steel by using ThermoCalc thermodynamic software and the database TCFE8, and speculated that the carbides should be **carburization**. Metallographic dataset of bearing steel available from Chen [13] is presented. This dataset is used by us to study the method proposed in this paper. Then, we compared the TUnet-CV model proposed in this paper with the current popular methods on three evaluation metrics to verify the effectiveness of the propos-

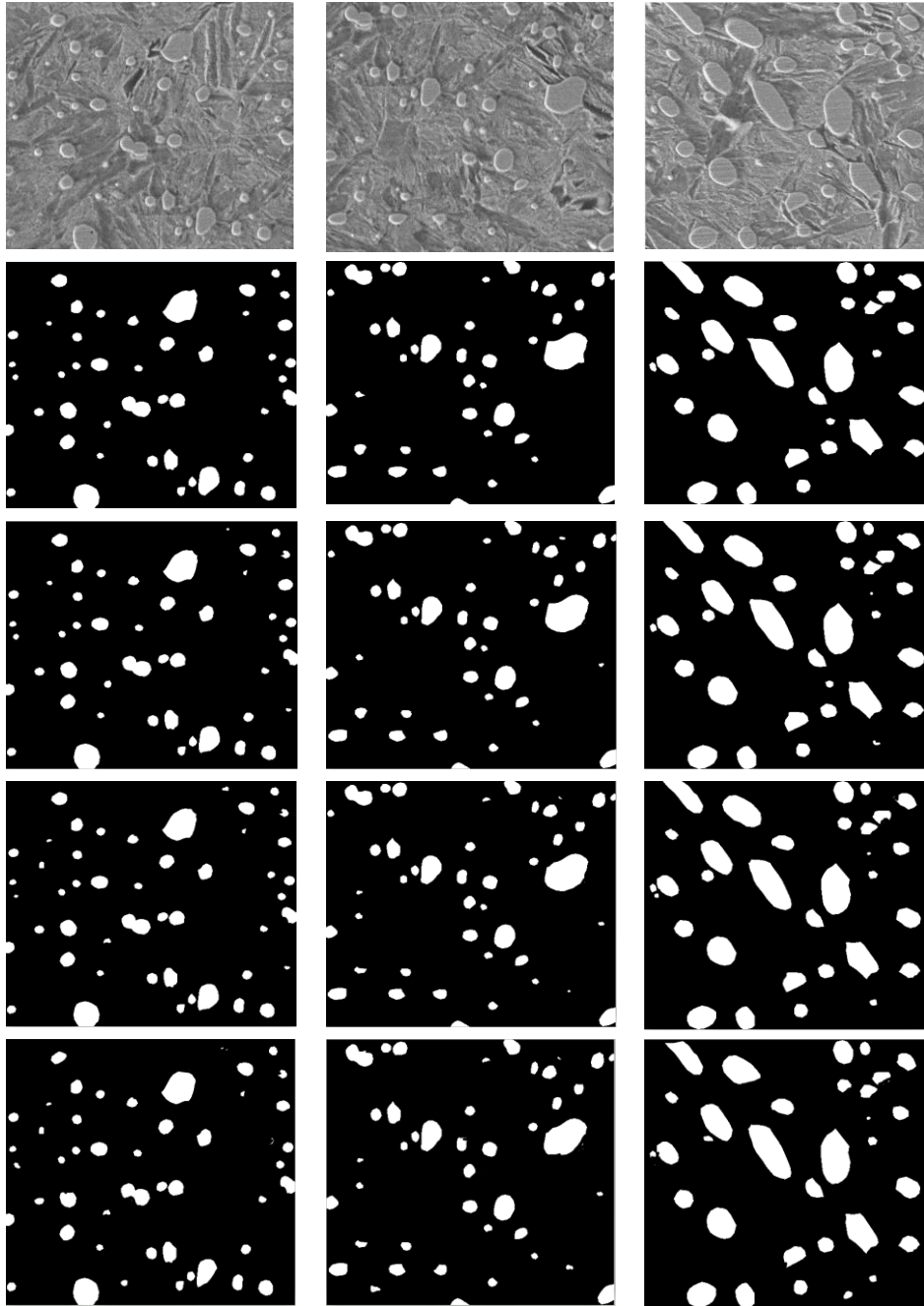


Fig. 4. Experimental results of TUNet-CV, TUNet and CV models are shown and compared.

ed algorithm. The image resolution is 512×512. The dataset is separated into two sets: training set and test set, where the training set contains 30 image samples and the test set contains 10 image samples. We perform data augmentation on the dataset to expand the training sample. The operations used include rotation, flipping and scaling. The training process of TUNet-CV model uses Adam optimizer with stochastic gradient descent strategy. The batch size is set to 1, the initial learning rate is set to 0.0001, and the learning rate decays 10 times every 3000 iterations for a total of 21000 iterations. The experimental computer CPU is Intel 4214R and the GPU is NVIDIA Tesla T4.

4.2 Evaluation metrics

In this paper three performance metrics are selected to measure: Dice coefficient, F1 measure and Precision. F1-measure is the harmonic average of accuracy and recall rate. Precision is the ratio of the total number of correct foreground pixels extracted to the total number of foreground pixels extracted by the segmentation result. Dice coefficient formula is as follows:

$$Dice = \frac{2(M \cap S)}{M + S} \quad (10)$$

M and S respectively represent the annotation data and the algorithm segmentation result.

4.3 Qualitative analysis of experimental results

We test the segmentation results of the TUNet-CV model in this paper on the metallographic dataset of bearing steel in Figure 4.

The first and second rows in Figure 4 show the training metallographic images and the corresponding label images for the datasets. The third row of Figure 4 shows the results of the segmentation of the selected test images by the TUNet-CV model. The results show that the method can effectively detect the carbides with small particle size while segment the lamellar carbons. The global and local scale information of bearing steel metallographic images are fully captured. The fourth row in Figure 4 shows the segmentation results of the TUNet model. It has the poor segmentation effect on the carbides with small particle size. The fifth row in Figure 4 shows the segmentation results of the CV model. By comparison, it can be seen that the proposed model in this paper performs better in segmentation effect.

4.4 Quantitative analysis of experimental results

Table I compares the results of the TUNet-CV model and the popular segmentation models in the metallographic diagram of bearing steel. Compared with other methods, TUNet-CV model achieved the highest Dice coefficient, F1 measure and Precision, reaching 0.9238, 0.9278 and 0.9115, respectively.

The morphology and distribution of the metallographic structure in the matrix material have great influence on the mechanical properties of the material. The carbon content of steel is one of the main factors affecting the properties of steel. Therefore, it is of great significance to analyze the content and size of insoluble carbides in the metallographic structure of GCr15 bearing steel.

Table 1. Comparison of the proposed method with other methods

Method	Dice coefficient	F1 measure	Precision
DeepLabV3+	0.8746	0.8980	0.8781
U-Gan	0.9158	0.9260	0.9096
Ostu	0.2647	0.2558	0.1610
Canny	0.3949	0.6400	0.6316
TUnet	0.8537	0.8931	0.8850
CV	0.7489	0.8245	0.8034
TUnet-CV	0.9238	0.9278	0.9115

In order to verify the effectiveness of the TUnet-CV model, controlled variable method is used to conduct ablation experiments. In Table 2, the U-net model, TUnet model, Unet-CV model and Tunet-CV model are tested on the bearing steel metallographic dataset. The Dice coefficient, F1 measure and Precision values of TUnet-CV model all reached the highest. Therefore, it is effectively proved that the Transformer module and the CV model in the fine segmentation stage introduced in this paper can effectively improve the segmentation result.

Table 2. Ablation experiments

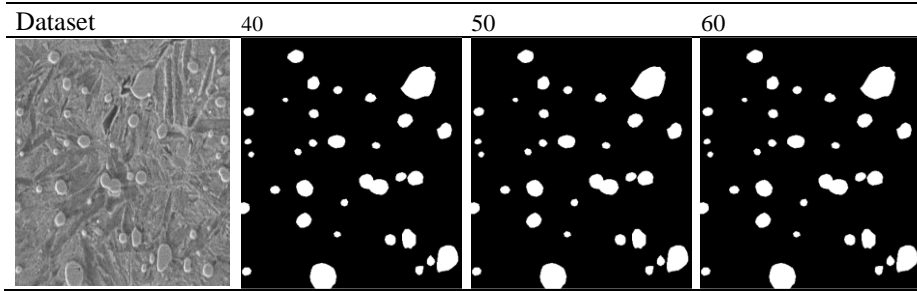
Method	Dice coefficient	F1 measure	Precision
U-net	0.6429	0.9046	0.8660
TUnet	0.8537	0.9151	0.8850
Unet-CV	0.8356	0.9075	0.8731
TUnet-CV	0.9238	0.9278	0.9115

We evaluate the effectiveness of the probability map as the initial contour by calculating the number of iterations required for the TUnet-CV model and CV model. The test results show that it takes 40 iterations on average to test the bearing steel image by TUnet-CV model. In contrast, testing the CV model required an average of 400 iterations. In this paper, we propose to use the probability map obtained by the TUnet model as the initial contour of the CV model, which significantly reduces the number of iterations and improves the efficiency compared with the CV model.

In Table 3, we conduct experiments on the relationship between stability and the number of iterations. We increase the average number of iterations of the TUnet-CV model by ten iterations, respectively, and the segmentation results are displayed to

show that the TUNet-CV model stabilizes at the average number of iterations. The segmentation results show that the TUNet-CV model is stable under the average number of iterations. Continuing to increase the number of iterations results in roughly consistent segmentation.

Table 3. Number of iterations and stability



5 Conclusion

In order to solve the problems of high similarity of gray values of various structures and complex topological structure in the metallographic image of the bearing steel, a two-stage segmentation model TUNet-CV for bearing steel is proposed in this paper. In the coarse segmentation stage, we select the TUNet network to segment the larger lamellar carbons and capture their complex topology. The coarse segmentation probability map obtained by the neural network is fed as a priori information to the fine segmentation stage. In the fine segmentation stage, the carbides with smaller particle size are finely segmented by a CV model with the probability map introduced as the initial contour. The proposed model is tested on the GCr15 bearing steel metallographic dataset. The experimental results demonstrate the validity of each component of the proposed model.

Acknowledgment

This work was supported by the Major Program of National Natural Science Foundation of China (72192830, 72192831), the 111 Project (B16009).

References

1. Domínguez-Rodríguez, JA González-Sánchez, Rosado-Carrasco J, et al. Grain Boundaries and Phases Identification of Metallographic Images by a Normalized Sobel Operation and the Edge Thinning Process for Further Numerical Simulation[J]. *Metals and Materials International*, 2019,26(9):1-12.

2. Cipolloni G, Menapace C, Cristofolini I, et al. A quantitative characterisation of porosity in a Cr–Mo sintered steel using image analysis[J]. *Materials Characterization*, 2014, 94:58-68.
3. Martyushev N V, Yu S V. The Method of Quantitative Automatic Metallographic Analysis [J]. *Journal of Physics: Conference Series*, 2017, 803:1-5.
4. Dutta T, Banerjee S, Saha S K, et al. Noise Removal and Image Segmentation in Micrographs of Ferrite-Martensite Dual-Phase Steel[J]. *Destech Transactions on Engineering and Technology Research*, 2017. 1-9.
5. Hecht M D, Webler B A, Picard Y N. Digital Image Analysis to Quantify Carbide Networks in Ultrahigh Carbon Steels[J]. *Materials Characterization*, 2016, 117:134-143.
6. Chan and Vese, Active contours without edges, *IEEE Transactions on image processing*, 10(2) (2001)266–277.
7. Naik D L, Sajid H U, Kiran R. Texture-based metallurgical phase identification in structural steels: asupervised machine learning approach[J]. *Metals*, 2019,9(5):54-56.
8. Kusche C, Reclik T, Freund M, et al. Large-area, high-resolution characterisation and classification of damage mechanisms in dual-phase steel using deep learning[J]. *PLOS ONE*, 2019,14(5):1-22.
9. Dimiduk D M, Holm E A, Niezgoda S R. Perspectives on the impact of machine learning, deeplearning, and artificial intelligence on materials, processes, and structures engineering[J]. *Integrating Materials and Manufacturing Innovation*, 2018,7(3):157-172.
10. Ronneberger O, Fischer P, and Brox T, U-net: Convolutional networks for biomedical image segmentation, *International Conference on Medical image computing and computer-assisted intervention*, Springer, (2015)234–241.
11. Youyang Sha Transformer-Unet: Raw image processing with Unet. arXiv preprint arXiv:2109.08417, (2021). Doi: 10.48550/arXiv.2109.08417
12. Mumford and J. Shah, Optimal approximations by piecewise smooth functions and associated variational problems, *Communications on pure and applied mathematics*, 42(5) (1989)577-685.
13. Chen Y, Jin W, Wang M. Metallographic image segmentation of GCr15 bearing steel based on CGAN[J]. *International Journal of Applied Electromagnetics and Mechanics*, 2020, 64(1-4):1237-1243.
14. Long J, Shelhamer E and Darrell, Fully convolutional networks for semantic segmentation, in: *IEEE Conference on Computer Vision and Pattern Recognition (CVPR)*, Boston, 2015, pp. 3431–3440.
15. Badrinarayanan V, Kendall A et al, SegNet: A deep convolutional encoder-decoder architecture for image segmentation, *IEEE Transactions on Pattern Analysis and Machine Intelligence* 39(12) (2017), 2481–2495.
16. He K, Gkioxari G, Dollár P et al. Mask R-CNN, in: *IEEE International Conference on Computer Vision (ICCV)*, Venice, 2017, pp. 2961–2969.
17. Chen L, Zhu Y, Papandreou et al. Encoder-decoder with atrous separable convolution for semantic image segmentation, in: *European Conference on Computer Vision (ECCV)*, Munich, 2018, pp. 801–818.
18. Simonyan K and Zisserman Z, Very deep convolutional networks for large-scale image recognition, in: *International Conference on Learning Representations (ICLR)*, San Diego, 2015.
19. Goodfellow I et al., Generative adversarial nets, *Advances in Neural Information Processing Systems* (2014), 2672–2680.

20. MA Chao, LUO Hai-wen. Precipitation and Evolution Behavior of Carbide During Heat Treatments of GCr15 Bearing Steel[J]. Journal of Materials Engineering, 2017, 45(6): 97-103.